ISSN 1996-5052

Current Research in Chemistry

Knowledgia SCIENTIFIC
A Place to Publish Outstanding Research

http://knowledgiascientific.com

Current Research in Chemistry 3 (2): 87-97, 2011
ISSN 1996-5052 / DOI: 10.3923/crc.2011.87.97

Electrochemical Study of Interaction of 3, 5-Ditertiarybutyl Catechol with Fe(III) Complexes of N-Salicylidene-L-Amino Acids

[1]Pradyut Sarma and [2]Okhil Kumar Medhi
[1]Department of Chemistry, Arya Vidyapeeth College, Assam, PIN-781016, India
[2]Department of Chemistry, Gauhati University, India

Corresponding Author: Okhil Kumar Medhi, Department of Chemistry, Gauhati University, India

ABSTRACT

Interaction of Iron (III) complexes of N-Salicylidene-L-amino Acids (i.e., [Fe(sal-L-his)]Cl.H_2O and [Fe (sal-L-ala)]Cl.H_2O) with catecholate substrate encapsulated in aqueous surfactant micelle has been projected as functional model of dioxygenase enzyme. Biomimetic environment for the study has been provided by the aqueous surfactant medium. Reaction of 3, 5-ditertiarybutyl catechol with the ferric complexes are studied elaborately by electrochemical techniques. These ferric complexes exhibit irreversible redox behaviour in aqueous as well as micellar medium, however, they are found to be quasi-reversible redox process in acetonitrile medium. Interaction of these complexes with 3, 5-ditertiary butyl catechol have shown by the presence of significant redox potential of semiquinone/catechol couple. The redox potential of semiquinone/catechol couple is more positive than that of the redox potential of free 3, 5-ditertiarybutyl catechol, it reflects stabilization of 3, 5-ditertiarybutyl catechol by chelation to ferric centre. Diffusion coefficient values of the catechol coordinated ferric complexes have been calculated and it found to be of the same order as those observed for other one electron reduction processes. The cyclic voltammogram of this interaction have recorded at various scan rates and it showed that this is a diffusion controlled redox process. All these observations provide support to the novel redox active pathway for modeling dioxygenase enzyme to convert phenolic substrates into less harmful aliphatic byproducts.

Key words: Cyclic voltammetry, osteryoung square wave voltammetry, diffusion coefficient, 3, 5-ditertiarybutyl catechol ($DBCH_2$), 3, 5-ditertiarybutyl semiquinone

INTRODUCTION

Iron is an essential element found in living system and its importance resides on its role as a protein active site constituent. Oxygen activating enzymes with mononuclear non-heme iron active sites participate in many metabolically important reactions that have environmental, pharmaceutical and medical significance (Ferraroni *et al*., 2006; Biegunki *et al*., 2010). Among the mononuclear iron enzymes catechol dioxygenase are the most important dioxygenase enzyme. Que and Reynolds (2000) as well as Costas *et al*. (2004) had categorically stated that catechol dioxygenase serves as part of nature's strategy for degrading catechol and poly catechols in the environment. They are mainly found in soil bacteria and act in the last step of transforming aromatic precursors into aliphatic products. Dioxygenase enzymes are known that contain heme iron, nonheme iron, copper or manganese. Catecholate 1,2- Dioxygenase (CTD) and

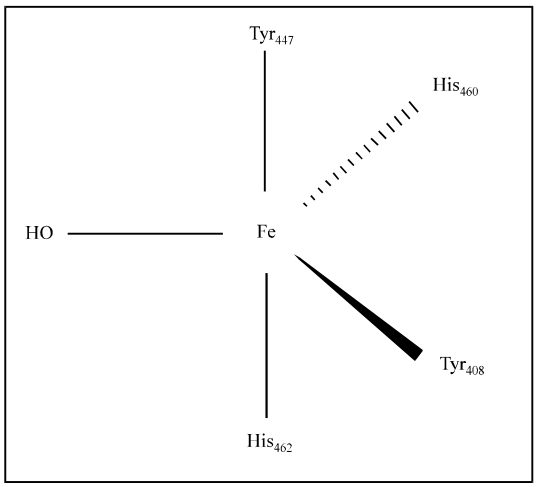

Fig. 1: Metal co-ordination sites of the crystallographically characterized iron enzyme (Protocatechuate 3,4-dioxygenase)

Protocatechuate 3, 4-Dioxygenase (PCD) are two important such bacterial non-heme iron enzymes. The substrates whose oxygenations are catalyzed by these enzymes are very diverse, as are the metal-binding sites; so probably several, possible unrelated, mechanisms operate in these different systems (Ohlendrof *et al.*, 1994; Horsman *et al.*, 2005; Fortin *et al.*, 2005; Mayilmurugan *et al.*, 2007).

Even before the X-ray crystal structure of PCD was obtained, a picture of the active site (Fig. 1) had been constructed by detailed spectroscopic work using a variety of methods. The two enzymes have different molecular weights and subunit composition but apparently contain very similar active site structures and functions by very similar mechanisms. In both, the resting state of the enzyme contains one Fe^{III} ion bound at the active site. EPR spectra show a resonance at g = 4.3, characteristic of high spin Fe^{III} in a so-called rhombic (low symmetry) environment and the Mossbauer parameters are also characteristic of high spin ferric. The crystal structure of the protocatechuate 3, 4-dioxygenase from *Pseudomonas aeruginose* reveals a trigonal bipyramidal iron site with four endogenous protein ligands (Tyr 447 and His 462 as the axial ligands and Tyr 408 and His 460 as the equatorial ligands). The third equatorial ligand is assignees to a solvent derived ligand. The iron active site sits at the end of a cleft with a hydrophobic channel that seems likely to be the substrate binding pocket (Hatta *et al.*, 2003; Miyazawa *et al.*, 2004). Very recently Paria *et al.* (2010), Dinelli *et al.* (2010) and Zeng *et al.* (2010) also highlighted a similar functional model of extradiol-cleaving dioxygenases.

This work is shaped to study the interaction of [Fe (sal-L-aa)] Cl complexs (aa = his and ala) with potential phenolate substrate like 3, 5-ditertiary butyl catechol ($DBCH_2$) in aqueous surfactant micelles, as models of catechol dioxygenases. The afford is directed towards investigating the reactivity and kinetics of the interaction of the ferric complexes with 3, 5-ditertiary butyl catechol by electrochemical methods. In this study, it has been tried to verify the validity of the proposed oxidative cleavage mechanism for the present Fe (III)-phenolate adduct. To correlate this work with biological systems all investigation were done in aqueous surfactant medium which could provide the hydrophobic as well as hydrophilic environment in this whole study (Ekpenyong and Antai, 2007; Abdurahman and Yunus, 2009).

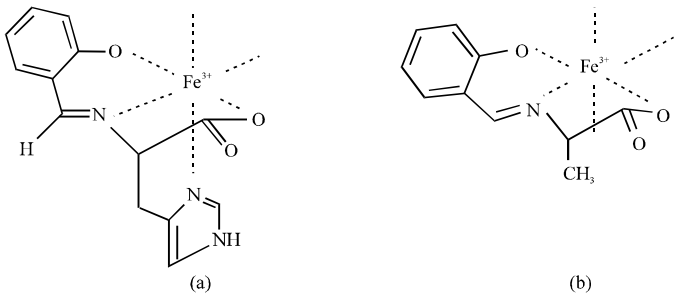

Fig. 2(a-b): Structure of (a) [Fe(sal-L-his)]Cl.H_2O and (b) [Fe(sal-L-ala)]Cl.H_2O

MATERIALS AND METHODS

Synthesis and characterization of [Fe(sal-L-aa)]Cl complexes (aa = his and ala): The complexes [Fe (sal-L-his)]Cl and [Fe(sal-L-ala)]Cl (Fig. 2) were prepared according to the already reported procedures (Casella *et al.*, 1987). All chemicals were purchased from Loba Chemie and used without further purification. The electronic spectra of the Fe (sal-L-aa) Cl complexes displayed several bands in the near-UV and visible regions; the absorption maxima in methanol or aqueous methanol solutions occurred near 228 nm (ε = 13000-18000 M^{-1} cm^{-1}), 256 nm (10000-15000 M^{-1} cm^{-1}), 288 nm (5000 M^{-1} cm^{-1}) and in the range 450-550 nm (1000-1400 M^{-1} cm^{-1}). The visible band was responsible for the purple colour of the complexes. Weak shoulder near 423 nm was always clearly detectable on the low energy tail of the 320 nm band. The spectra showed solvent dependence; this was partly due to solvent coordination to iron (III) but was also due to a different degree of association of the complexes in the various solvents. The spectra of Fig. 2a and b in protic solvents often show significant concentration dependence, the visible band being mostly affected in these conditions. IR spectra of the complexes hinted ν (OH) band at 3000-3300 cm^{-1} and imine structure of the ligands account for intense and well resolved ν (C = N) bands near 1590-1610 cm^{-1}. Band at 1300-1330 cm^{-1} indicated ν (O-Ph) stretching.

Electrochemical analysis: Cyclic voltammery is the most widely used technique for acquiring information about electrochemical reactions. The power of cyclic voltammetry results from its ability to rapidly provide considerable information on thermodynamics of redox processes and the kinetics of heterogeneous electron-transfer reactions, and on coupled chemical reactions or adsorption processes. Cyclic Voltammetry (CV) is often the first experiment performed in an electro analytical study. In particular, it offers a rapid location of redox potentials of the electropositive species and convenient evaluation of the effect of medium upon the redox process. The values of $E_{1/2}$ are determined by cyclic voltammetry can confirmed by further measurement by the relatively new technique in electrochemical analysis, namely Osteryoung Square Voltammetry (OSWV). Electrochemical experiments are performed on a BAS model 100A electrochemical analyzer. Bio Analytical system; USA. A three electrode cell assembly with Nitrogen gas purging lines was used in combination with the analyzer. The working electrode is glassy carbon, reference electrode is Ag-AgCl electrode and platinum electrode is used as auxiliary electrode. The supporting electrolyte is $NaNO_3$ about 100 times the concentration of the electroactive species. The reference electrode potential was calibrated by measuring the $E_{1/2}$ of the ferrocene/ferrocinium couple in acetonitrile.

Diffusion coefficient: Diffusion coefficient (D_0) is a factor of proportionality representing the amount of substance diffusing across a unit area through a unit concentration gradient in unit

time. It is a significant parameter to categories the reaction dynamics of redox processes in electrochemical analysis.

The values of diffusion coefficient (D_0) of $DBCH_2$ coordinated $[Fe(sal\text{-}L\text{-}aa)]^+$ adducts in aqueous surfactant micelles were calculated by substituting the slope obtained from the linear i_{pc} vs. $\nu^{1/2}$ (ν<0.05 Vs^{-1}) plot in the Randles- Sevcik equation (Das and Medhi, 1998; Bard and Faulkner, 2006).

$$i_p = 2.69 \times 10^5 \, n^{3/2} \, ACD^{1/2} \, \nu^{1/2}$$

Where:

i_p = Peak current (A) n = Number of electrons transferred
A = Electrode surface area (cm^2) C = Concentration (mol cm^{-1})
D = Diffusion coefficient (cm^2s^{-1}) ν = Sweep rate (Vs^{-1})

UV-visible spectra were recorded in a Hitachi U-3210 model as well as in Perkin Elmer Lambda 40 uv/vis spectrometer. The oxygenation kinetics experiments were performed in a 10 mm path length Thunberg quartz cuvette. pH dependent measurements were made by Adair Dupp. and Co. India) model number DPH- 77 pH meter. The pH electrode was SCE glass combined electrode which was standardized with known buffer solution. IR spectra was recorded a Perkin Elmer RXIFT - IR spectrophotometer. We used cationic micelle Cetyltrimethyl Amonium Bomide (CTAB), anionic micelle Sodiumdodecy Sulphate (SDS) and neutral micelles polyethylene glycol p-(1, 1, 3, 3-tetramethylbutyl)-phenyl ether (TritonX-100) in our experiments. In this study we have used different concentrations of the surfactant micellar solutions and they are 2%, 4% and 3% for SDS, CTAB and TritonX- 100, respectively. These micellar concentrations are adjusted above the level of the critical micellar concentration (Bari *et al.*, 2009; Gokturk and Var, 2011). It favors the complete micellization of the complex and also reduce the chance of any change in mid point redox potential value due to any minor fluctuation in the micelle concentration.

RESULTS AND DISCUSSION

Complexes in Fig. 2 were highly soluble in water and also in aqueous surfactant medium. However the redox potential of Fe^{3+}/Fe^{2+} couple for the complexes were different in aqueous and aqueous surfactant solutions. When these complexes got dissolved in aqueous solution the fifth position around the Fe centre of the active site got occupied by H_2O molecule and actual formula of the complexes become $[Fe\ (sal\text{-}L\text{-}his)\ H_2O]^+$ and $[Fe\ (sal\text{-}L\text{-}ala)\ H_2O]^+$ (Casella *et al.*, 1987). The midpoint potential ($E_{1/2}$) of the complex $[Fe\ (sal\text{-}L\text{-}his)]^+$ in aqueous medium was -0.120 V. But in aqueous micellar medium these $E_{1/2}$ values had shifted towards more negative potential, for example $[Fe(sal\text{-}L\text{-}his)]^+$ had $E_{1/2}$ values at -0.236 V in SDS micelle, -0.400 V in CTAB micelle and -0.182 V in TritonX-100 micelle. Similar sort of variation of $E_{1/2}$ values were also observed for complex $[Fe\ (sal\text{-}L\text{-}ala)]^+$, e.g. in aqueous medium the $E_{1/2}$ of the complex was -0.213 V whereas in SDS micelle the value was -0.601 V, in CTAB micelle it was -0.360 V and in TritonX-100 micelle $E_{1/2}$ was -0.411 V. More negative values of $E_{1/2}$ in micellar medium compared to that of the aqueous solution hinted the grater stabilization of Fe^{III} centre in micellar medium towards reduction.

Complexes in Fig. 2 are also soluble in acetonitrile. 3×10^{-3} molar solution of complex (Fig. 2b) in acetonitrile had prepared and its cyclic voltammetric response had investigated. A cyclic voltammogram with similar height of cathodic and anodic peak had produced (Fig. 3). The mid

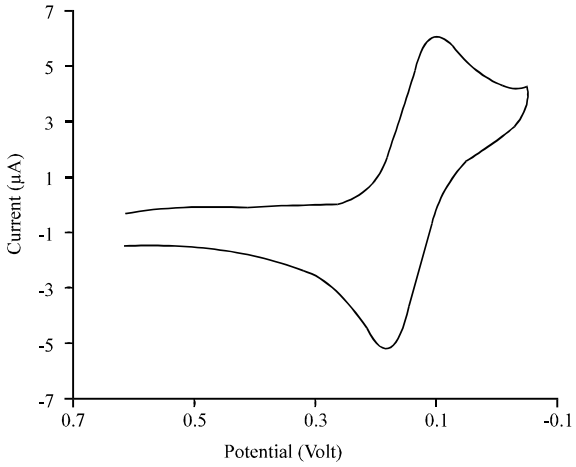

Fig. 3: Cyclic Voltammogram of complex $[Fe(sal\text{-}L\text{-}ala)]^+$ in acetonitrile solution

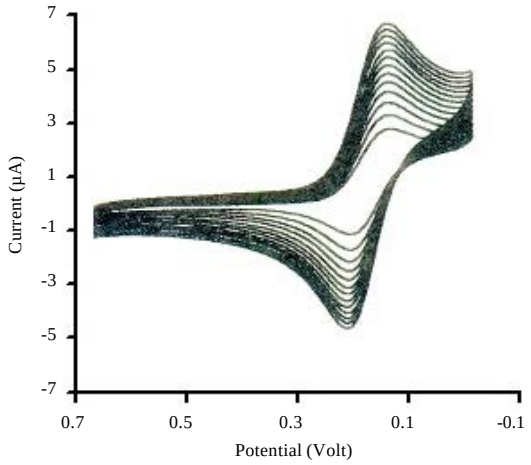

Fig. 4: Scan rate dependent cyclic voltammetry of $[Fe(sal\text{-}L\text{-}ala)]^+$ in acetonitrile solution

point potential ($E_{1/2}$) of complex (Fig. 2b) (i.e., $[Fe\ (sal\text{-}L\text{-}ala)]^+$) was found to be 0.159 V. This Cyclicvoltammetric (CV) response was recorded at scan rate 0.1 Vs^{-1} with peak separation ΔE_p = 70 mV. Similarly Cyclic Voltammetry (CV) of complex (Fig. 2a) ($[Fe(sal\text{-}L\text{-}his)]^+$) also recorded in acetonitrile medium and the $E_{1/2}$ value was measured as 0.150V with peak separation ΔE_p = 111 mV. Cyclic voltammetric response is significantly based on its scan rate (represented by **ν**). If we recorded different cyclic voltammogram at different scan rates for the same complex: $[Fe(sal\text{-}L\text{-}his)]Cl.H_2O$ or $[Fe(sal\text{-}L\text{-}ala)]Cl.H_2O$ then it showed the peak separation ΔE_p for each graph was nearly constant for lower scan rate and it was gradually increasing with increasing scan rate (Fig. 4). Current function $i_{pc}/\sqrt{\nu}$ increase with increasing scan rate and i_{pc}/i_{pa} ratios was 1.23 and 0.97, respectively. All these results indicated that these redox systems were quasi-reversible. These results are consistent with the redox process of other ferric complexes involving one electron reduction reaction (Das *et al.*, 1997; Bard and Faulkner, 2006).

Interaction of $DBCH_2$ with [Fe(sal-L-his)]Cl and [Fe(sal-L-ala)]Cl in surfactant medium: Interaction of 3, 5-ditertiary butyl catechol ($DBCH_2$) with $[Fe\ (sal\text{-}L\text{-}aa)]^+$ complexes (aa = his and

ala) could easily be interpret by the electrochemical analysis. $[Fe\ (sal\text{-}L\text{-}aa)]^+$ complexes exhibited irreversible cyclic voltammogram but when it got coordinated with $DBCH_2$ at appropriated pH level, a new oxidation wave appeared and it corresponding to the DBSQ/$DBCH_2$ couple. Interaction of $DBCH_2$ with metal centre required special pH condition, at low pH value (≈ 7-8.5) its first proton got departure from OH group and $DBCH_2$ became $DBCH^-$. At this stage $DBCH^-$ is available for monodentate coordination with ferric complexes. On the other hand, as pH value increased, (≈ 10-11.5), proton of next OH group of $DBCH^-$ got deprotonated and it became DBC^{2-} i.e., ready for bidentate coordination with ferric complexes. These coordination possibilities of 3, 5-ditertiary butyl catechol has shown in Fig. 5. These sort ligand stereoelectronic properties are also observed during interaction of $DBCH_2$ with Fe (III) complexes of tetradentate monophenolate ligands (Velusamy *et al*., 2004).

These facts were well furnished by the following potential values: 3×10^{-3} mol amount of $[Fe\ (sal\text{-}L\text{-}his)]^+$ and equivalent amount of $DBCH_2$ had dissolved in SDS surfactant solution. To this mixture 2 equivalent of base (NaOH) was added and the pH had increases to 7-8.5 and it favoured the monodenated coordination of 3, 5-ditertiary butyl catechol with $[Fe\ (sal\text{-}L\text{-}his)]^+$ complexes which became [Fe(sal-L-his)DBCH] adduct. $E_{1/2}$ of this [Fe(sal-L-his)DBCH] adduct was -0.175 V. To the same solution when we had added again two equivalents of base and the pH level increased to 10-11.5 and consequently $DBCH^-$ became DHC^{2-} which was ready to coordinate with ferric centre by bidentate mode i.e., $[Fe\ (sal\text{-}L\text{-}his)DHC]^-$ adduct. $E_{1/2}$ of this bidentate complex adduct was -0.125 V.

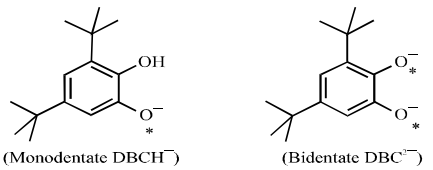

Fig. 5: Possible coordination of 3,5-ditertiarybutyl catechol with metal centre

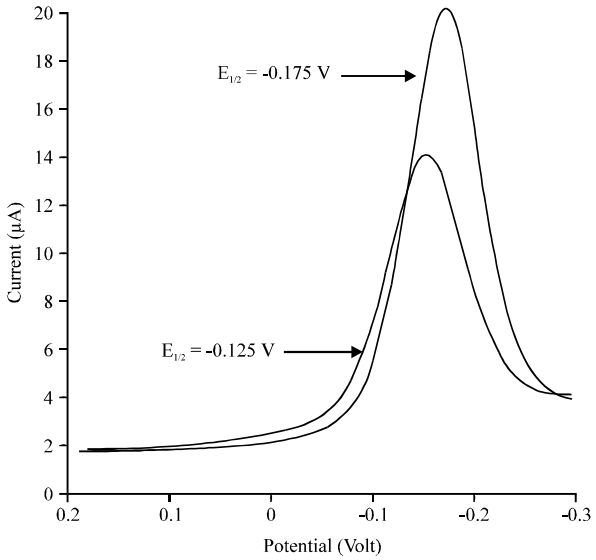

Fig. 6: Osteryoung square wave voltammetry (OSWV) of monodentate [Fe(sal-L-his)DBCH] and $[Fe(sal\text{-}L\text{-}his)DBC]^-$ adduct in SDS micelle

Table 1: Electrochemical data for the $DBCH_2$ coordinated ferric complexes

Complex	Solvents	pH	$E_{1/2}$ (V)	ΔE_p (mV)	i_{pc}/i_{pa}	Do($\times10^{-11}$)(cm^2sec^{-1})
[Fe(sal-L-his) HDBC]	SDS	8.0	-0.175	87	1.20	138.10
	CTAB	8.0	-0.070	82	1.34	6.10
	TritonX-100	8.0	-0.185	92	1.30	2.30
[Fe(sal-L-his) DBC]$^-$	CH_3CN	11.5	0.152	57	1.80	111.80
	SDS	11.5	-0.125	85	1.20	95.10
	CTAB	11.5	0.030	68	1.31	1.20
	TritonX-100	11.5	-0.115	73	1.21	0.88
[Fe(sal-L-ala) HDBC]	CH_3CN	8.0	0.175	94	1.33	25.30
	SDS	8.0	-0.160	102	1.19	24.90
	CTAB	8.0	-0.176	140	1.30	0.859
	TritonX-100	8.0	-0.152	94	1.30	198.00
[Fe(sal-L-ala) DBC]$^-$	CH_3CN	11.5	0.234	99	1.26	45.60
	SDS	11.5	-0.095	120	1.41	6.20
	CTAB	11.5	-0.065	75	1.30	0.56
	TritonX-100	11.5	-0.120	95	1.25	12.10

i_{pc} and i_{pa} are the cathodic peak current and anodic peak current, respectively. D_0 is the diffusion coefficient of the respective species

Their peak currents were i_{pc} (cathodic current) 4.15×10^{-6} ampere and i_{pa} -4.05×10^{-6} ampere. By comparison it was evident that [Fe(sal-L-his) DBC]$^-$ (bidentate coordination) had $E_{1/2}$ value more positive than that of [Fe(sal-L-his)DBC]$^-$ momodentate adduct (Table 1). It revealed that DBC^{2-} coordinated in bidentate mode in the former case was more stabilized towards oxidation that of the latter case (Fig. 6).

The potential required for oxidation of free 3, 5-ditertiary butyl catechlol ($DBCH_2$) was -0.890V and when it coordinated with ferric centre, either in monodenate or bidentate fashion, it got shifted toward positive potential (i.e., -0.175 and -0.125 V). It reflected the considerable stabilization of $DBCH_2$ from oxidation by chelation to ferric centre. Velusamy and Palaniandavar (2003), Wang *et al.* (1997) and Chiou and Que (1995) had also worked in this field and they too highlighted similar type of positive shifting of $E_{1/2}$ values after coordination with chelating ligand. $E_{1/2}$ of catecholate bound adducts were more positive than that of the redox potential of the parent complex and it reflects the Lewis acidity of the iron centre in [Fe (sal-L-aa) DBC]$^{n-}$ which decreases with the increase in number of co-ordinated phenolate groups. These results were also supported by Lauffer *et al.* (1983) and Nanni *et al.* (1980).

We had recorded the cyclic voltammograms of bidentate adducts [Fe (sal-L-his) DBC]$^-$ and [Fe (sal-L-ala) DBC]$^-$ at different scar rate. These scan rate dependent cyclic voltammetric response for [Fe (sal-L-ala) DBC]$^-$ adduct in the CTAB micellar medium was shown in Fig. 7. For these voltammograms, at slow scan rate the peak current ratio $i_{pc}/\sqrt{v}$ was linear and independent of scan rate; peak current i_{pc} and i_{pa} were linearly proportional to the square root of scan rate as shown in Fig. 8. These electrochemical results indicated that Fe^{3+}/Fe^{2+} redox process of the catecholate adduct of Fe (III) complexes in surfactant micelles was a diffusion controlled quasi-reversible electron transfer process (Das *et al.*, 1997; Das and Medhi, 1998).

The values of current function ($D_0 = 0.56\times10^{-11}$ - 138.1×10^{-11} cm^2 sec^{-1}) of the ferric complexes were of the same order as those observed for other iron (III) complexes undergoing a one electron reduction process. These values were also listed in Table 1 and it was evident that diffusion constants of the complexes were lowered in micellar medium. This was might be because of the high viscosity provided by the micellar medium. Nematollahi *et al.* (2010),

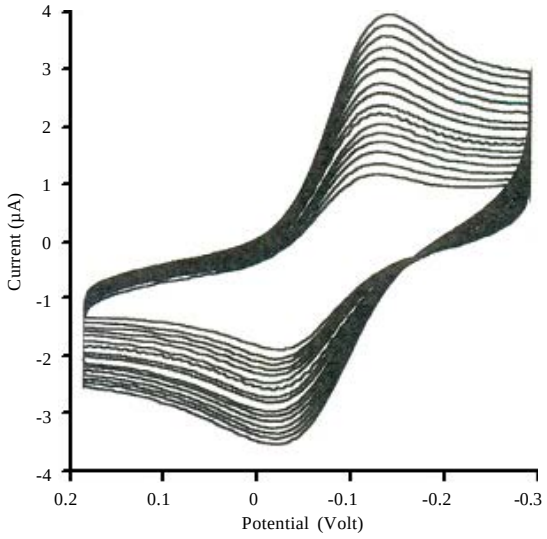

Fig. 7: Scan rate dependent cyclic voltammograms of [Fe(sal-L-ala)DBC] adduct in CTAB micelle

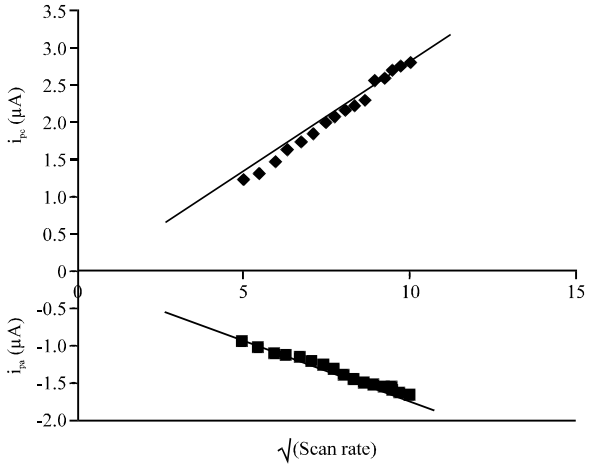

Fig. 8: Plot of peak currents (i_{pc} and i_{pa}) vs the square root of the scan rate of $[Fe(sal\text{-}L\text{-}ala)DBC]^{-}$ adduct in CTAB micelle

Dhanalakshmi *et al.* (2006), Mayilmurugan *et al.* (2007) and Viswanathan *et al.* (1996) had also reported many works in this field and their work supported these range of diffusion coefficient values for Fe^{3+} Fe^{2+} reduction processes. The i_{pc} vs $\nu^{1/2}$ plot is linear but the values of peak current ratio i_{pa}/i_{pc} (1.0-0.6) and the peak potential separation ΔE_p (69-140 mV) suggest fairly reversible to irreversible redox processes.

CONCLUSION

The redox potential of metal bound DBSQ/H_2DBC couple is significantly more positive than that of free H_2DBC, reflecting considerable stabilization of H_2DBC by chelation to ferric centre. Also it is more positive than that of the Fe (III)/Fe (II) couple of the parent complex and reflects the lewis acidity of the iron centre in $[Fe(L)DBC]^{n-}$ which decreases with the increases in number of coordinated phenolate groups.

It is well known that phenolic waste products from paper industries and oil refineries cause a major threat to surrounding areas. Afford to work out proper redox environment for the conversion of toxic phenolic products into less toxic aliphatic byproducts would be of great significanc. Knowledge of proper redox behavior for such [Fe (sal-L-aa)]-$DBCH_2$ interaction would be a right step to construct devices which can accomplished the conversion of toxic phenolate substrate into less toxic aliphatic byproducts.

ACKNOWLEDGMENT

We thank the University Grant Commission, New Delhi, for supporting this research work during the period 2007-2009 (No.F.5-294/2007-08 (MRP/NERO)/1464). The researchers wish to acknowledge the Head of the department, department of chemistry, Gauhati University, for providing the facilities to accomplish the project work.

REFERENCES

Abdurahman, H.N. and R.M. Yunus, 2009. Coalescence of water droplets in water-in-crude oil emulsions. Int. J. Chem. Technol., 1: 19-25.

Bard, A.J. and L.R. Faulkner, 2006. Electrochemical Methods, Fundamentals and Applications. 2nd Edn., Wiley India Pvt. Ltd, New Delhi, ISBN: 81-265-0807-8, pp: 226-256.

Bari, H.A.A., R.B.M. Yunus, W.K. Mahmood and Z.B. Hassan, 2009. Sodium stearate as drug reducing agent in Non Aqueous medium. Int. J. Chem. Technol., 1: 11-18.

Biegunki, A., A. Frydrychewicz, M. Osial and K. Jackowska, 2010. Electrochemical oxidation of catechol at poly(indo-5-carboxylic acid) electrode. Russ. J. Electrochem., 46: 1297-1305.

Casella, L., M. Gullotti, A. Pintar, L. Messori, A. Rockenbauer and M. Gyor, 1987. Coordination modes of histidine. 10. Iron (III) tyrosinate models. Synthesis and spectroscopic and stereochemical studies of iron (III) complexes of N-salicylidene-L-amino acids. Inorg. Chem., 26: 1031-1038.

Chiou, Y.M. and Jr. L. Que, 1995. Structure of a mononuclear iron (II)-catecholate complex and its releavance to the extradiol-cleaving catechol dioxygenases. Inorg. Chem., 34: 3577-3578.

Costas, M., M.P. Mehn, M.P. Jensen and Jr. L. Que, 2004. Dioxygen activation at mononuclear nonheme iron active sites: Enzymes, models and intermediates. Chem. Rev., 104: 939-986.

Das, D.K., C. Bhattaray and O.K. Medhi, 1997. Electrochemical behaviour of (protoporphyrinato IX) iron (III) encapsulated in aqueous surfactant micelles. J. Chem. Soc., Dalton Trans., 1997: 4713-4718.

Das, D.K. and O.K. Medhi, 1998. Effect of surfactant and pH on the redox potential of microperoxidase 11 in aqueous micellar solutions. J. Chem. Soc., Dalton Trans, 1998: 1693-1698.

Dhanalakshmi, T., M. Bhuvaneshwari and M. Palaniandavar, 2006. Iron (III) complexes of certain meridionally coordinating tridentate ligands as models for non-heme iron enzymes: The role of carboxylate coordination. J. Inorg. Biochem., 100: 1527-1534.

Dinelli, L.R., T.M.S. Bezerra and J.J. Sene, 2010. A kinetic study of the reaction between *trans*-$[CoCl_2(en)_2]Cl$ and the amino acids alanine and valine. Curr. Res. Chem., 2: 18-23.

Ekpenyong, M.G. and S.P. Antai, 2007. Influence of pH on cadmium toxicity to bacillus species (02 and 12) during biodegradation of crude oil. Int. J. Biol. Chem., 1: 29-37.

Ferraroni, M., I.P. Solyanikova, M.P. Kolomytseva, A. Scozzafava, L. Golovleva and F. Briganti, 2006. Crystal structure of 4-chlorocatechol 1,2- dioxygenase from the chlorophenol-utilizing gram-positive *Rhodococcus opacus* 1CP. The J. Biolog. Chem., 279: 27646-27655.

Fortin, P.D., I. Macpherson, D.B. Neau, J.T. Bolin and L.D. Eltis, 2005. Directed evolution of a ring-cleaving dioxygenase for polychlorinated biphenyl degradation. J. Biol. Chem., 280: 42307-42314.

Gokturk, S. and U. Var, 2011. Effect of ethanol on partition and binding equilibrium of phenothiuzine in anionic and nonionic micellar solution. Curr. Res. Chem.,

Hatta, T., G. Mukerjee-Dhar, J. Damborsky, H. Kiyohara and K. Kimbara, 2003. Characterization of a novel thermostable Mn(II)-dependent 2,3-dihydroxybiphenyl 1,2-dioxygenase from a PCB and naphthalene-degrading *Bacillus* sp. JF8. J. Biol. Chem., 278: 21483-21492.

Horsman, G.P., A. Jirasek, F.H. Vaillancourt, C.J. Barbosa and A.A. Jarzecki *et al.*, 2005. Spectroscopic studies of the anaerobic enzyme-substrate complex of catechol 1,2-dioxygenase. J. Am. Chem. Soc., 127: 16882-16891.

Lauffer, R.B., R.H. Heistand and Jr. L. Que, 1983. Dioxygenase models. Dioxygenase models. Crystal structures of the 2,4-pentanedionato, phenanthrene semiquinone and catecholato complexes of N,N'-ethylenebis(salicylideneaminato) iron (III). Inorg. Chem., 22: 50-55.

Mayilmurugan, R., S. Eringathodi and P. Mallayan, 2007. A new tripodal Iron (III) monophenolate complex: Effects of ligand basicity, steric hindrance and solvent on regioselective extradiol cleavage. Inorg. Chem., 46: 6038-6049.

Miyazawa, D., G. Mukerjee-Dhar, M. Shimura, T. Hatta and K. Kimbara, 2004. Genes for Mn(II)-dependent NahC and Fe(II)-dependent NahH located in close proximity in the thermophilic naphthalene and PCB degrader, *Bacillus* sp. JF8: Cloning and characterization. Microbiology, 150: 993-1004.

Nanni, Jr. E.J., M.D. Stallings and D.T. Sawyer, 1980. Does superoxide ion oxidize catechol,.alpha.-tocopherol and ascorbic acid by direct electron transfer? J. Am. Chem. Soc., 102: 4481-4485.

Nematollahi, D., A. Taherpour, S.J. Bozorghi, A. Mansouri and B. Dadpou, 2010. Experimental and computational study on electrochemical oxidation of catechols. Int. J. Electrochem. Sci., 5: 867-879.

Ohlendrof, D.H., A.M. Orville and J.D. Lipscomb, 1994. Structure of procatechuate 3, 4-dioxygenase from *Pseudomonas aeruginosa* at 2015 A^0 resolution. J. Mol. Biol., 244: 586-608.

Paria, S., P. Halder and T. Painepp, 2010. A functional model of extradiol-cleaving Dioxygenases: Mimickimg the 2-His-1-Carboxylate Facial triad. Inorg. Chem., 49: 4518-4523.

Que, Jr. L. and M.F. Reynolds, 2000. Manganese(II)-dependent extradiolcleaving catechol dioxygenases. Met. Ions Biol. Syst., 37: 505-525.

Velusamy, M. and M. Palaniandavar, 2003. Novel iron (III) complexes of tripodal and linear tetradentate bis(phenolate) ligands: Close relevance to intradiol-cleaving catechol dioxygenases. Inorg. Chem., 42: 8283-8293.

Velusamy, M., R. Mayilmurugan and M. Palaniandavar, 2004. Iron(III) complexes of sterically hindered tetradentate monophenolate ligands as functional models for catechol 1,2-dioxygenases: The role of ligand stereoelectronic properties. Inorg. Chem., 43: 6284-6293.

Viswanathan, R., M. Palaniandavar, T. Balasubramanian and P.T. Muthiah, 1996. Synthesis, structure, spectra redox of iron (III) complexes of tridentate pyridyl and benzomidazolyl ligands. J. Chem. Soc., Dalton Trans., 1996: 2519-2525.

Wang, S., L. Wang, X. Wang and Q. Luo, 1997. Synthesis, characterization and crystal structure of a new tripodal ligand containing imidazole and phenolate moieties and its iron (III) complexes. Inorg. Chim. Acta, 254: 71-77.

Zeng, C. C., D. W. Ping, l. M. Hu, X. Q. Song and R. G. Zhong, 2010. Anodic oxidation of catechols in the presence of alpha-oxoketene N,N-acetals with a tetrahydropyrimidine ring: selective alpha-arylation reaction. Org. Biomol. Chem., 8: 2465-2472.